

Sedimentation Pattern in a Macrotidal Bay (Namhaepo Bay), West Coast of Korea

SANG-DO LEE AND SOO-CHUL PARK

Department of Oceanography, Chungnam National University, Taejon 305-764, Korea

한국 서해안 대조차 만(남해포만)에서의 퇴적양상

이상도 · 박수철

충남대학교 해양학과, 대전, 305-764

The sedimentation pattern in Namhaepo Bay, a macrotidal coastal embayment of western Korea, was investigated by means of analysing high-resolution seismic profiles, sediment samples, and tidal currents. Recent sediments up to 20 m thick overlie the irregular surface of the acoustic basement. The sediments consist mainly of sandy silt and silt; the mean grain size of these sediments ranges from 4 to 5.5 ϕ , showing a shoreward-fining distribution pattern. This distribution pattern agrees with the directions of tidal currents in the bay, which flow N-NE (shoreward) during flood and are largely reversed during ebb, with a maximum velocity of 39 cm/sec. The calculated shear velocity of the tidal currents at sea bed ranges from 0.5 to 3.3 cm/sec during flood and from 0.7 to 2.5 cm/sec during ebb. The mean values of these velocities exceed the critical shear velocity for the silt particles. The data suggest that the tidal currents play an important role in the transportation and deposition of sediments in the bay and the surface topography of the sea floor is largely determined by tidal sedimentation.

고정밀 탄성파자료, 퇴적물시료, 조류를 분석하여 한국서해안 대조차 지역인 남해포만에서의 퇴적양상을 조사하였다. 만에서의 현생퇴적층의 두께는 약 20m에 달하며 불규칙적인 음향기반암을 덮고 있다. 퇴적물은 주로 사질 실트나 실트로 구성되어 있으며, 평균입도는 4-5.5 ϕ 의 범위이고 해안선을 향하면서 세립화하는 경향을 보인다. 이러한 분포양상은 만에서의 조류의 운동방향과 잘 일치한다. 해저면에서의 조류의 전단속도는 창조시 0.5-3.3 cm/sec, 낙조시 0.7-2.5 cm/sec의 범위를 보이며, 이러한 전단속도들의 평균값은 만내에 분포하는 실트입자를 재동하거나 운반할 수 있는 임계전단속도 값을 능가한다. 이러한 자료들은 조류가 만내에 분포하는 퇴적물 입자들의 이동과 퇴적에 중요한 역할을 하며, 해저면의 표층지형은 주로 조석퇴적작용에 의하여 결정되었음을 시사해 준다.

INTRODUCTION

The western coast of the Korean Peninsula is occupied by many coastal embayments related to the post-glacial transgression. This area is generally considered as a depositional environment dominated by tidal sedimentation. The large tidal range (up to 9 m) and resulting tidal currents produce a complex and dynamic hydraulic regime

in terms of sediment erosion and deposition (Song *et al.*, 1983; Bloom and Park, 1985; Adams *et al.*, 1990). However, relatively little attention was paid to the relationship between the tidal currents and bottom sediment distribution. This paper aims at understanding the bottom shear stress and sediment types to evaluate the sedimentation pattern in a small macrotidal bay (Namhaepo Bay) (Fig. 1).

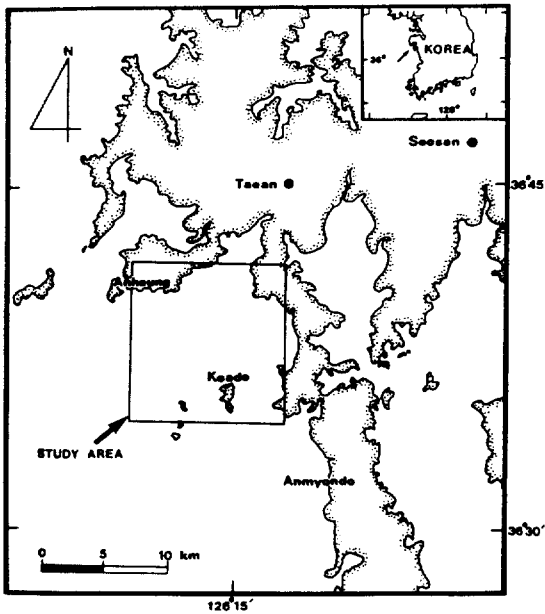


Fig. 1. Index map showing the study area.

STUDY AREA

Namhaepo Bay is a shallow coastal embayment on the ria-type western coast of the Korean Peninsula (Fig. 1). This area is part of the Seosan National Marine Park which extends about 30 km to the north and to the south along the coast. The bay is surrounded by an irregular, rocky coast which has relatively low relief to the north and east, whereas it is open to the Yellow Sea to the southwest. The bay is characterized by a semi-diurnal tide with the maximum tidal range up to 650 cm (Korea Hydrographic Office, 1989). Major flood and ebb currents trend NE-SW with current velocities of 40 to 70 cm/sec offshore. Wind directions in the study area are seasonally bimodal. Winds blow predominantly from the southwest in summer and from the northwest in winter (National Geographic Institute of Korea, 1980). The adjacent land geology mainly consists of Precambrian metamorphic rocks such as schist, quartzite and gneiss, which are intruded by Jurassic granite (Korea Institute of Energy and Resources, 1981). These rocks extend seaward and form the basement rocks of the nearcoastal area.

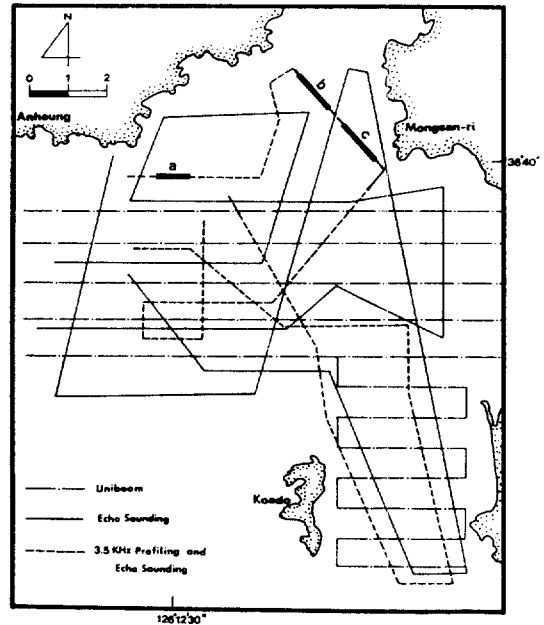


Fig. 2. Tracklines of Uniboom profiles, echo-sounding and 3.5 kHz profiling (a, b, and c indicate profiles shown in Fig. 4).

MATERIALS AND METHODS

Fifty-four bottom sediment samples were collected with a Dietz-Lafond grab sampler from a small boat in February and April, 1989. Positioning was maintained by radar and sextant. The grain size of sediment samples was determined by a standard sieving technique for the sand fraction and by a pipette method for the mud fraction. High-frequency subbottom profiles were collected with an 3-7 kHz ORE pinger system, while a Raytheon model DE-719B (208 kHz) fathometer was used for bathymetry (Fig. 2). High-resolution Uniboom profiles, previously collected by the National Geographic Institute of Korea (1980) were also examined in this study to interpret the subsurface structure.

Tidal currents were measured at three stations during spring tide (Fig. 3). Data were obtained with a Toho-Dentan CM-2 direct reading current meter at 0.5 m above the sea bed, and successively at 0.5 m interval up to the sea surface. Because of Korean navigation security regulations, we were

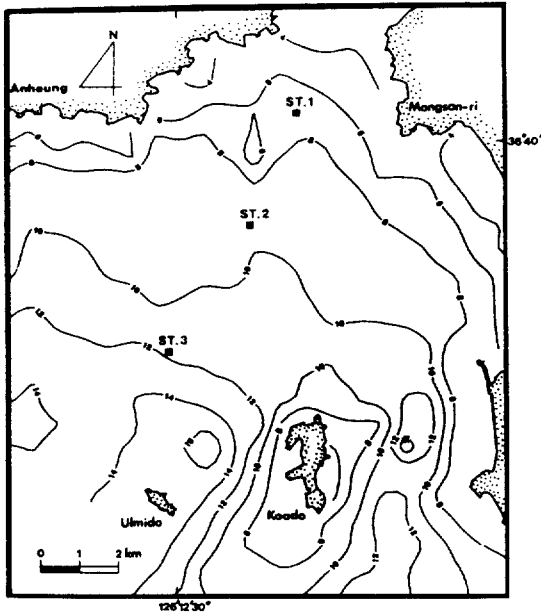


Fig. 3. Bathymetry of the study area compiled from the echosounding data (contours in meters below mean sea level). Large numbers (ST. 1, ST. 2 and ST. 3) indicate stations of tidal current measurement.

not able to occupy two stations (stations 1 and 2) longer than 10 hours. The tidal range was 528 cm when the current was measured. The tidal current data were used for calculation of bottom shear velocity and shear stress.

BATHYMETRY AND SUBSURFACE GEOLOGY

Sounding data from different times of flood and ebb tide were corrected in terms of mean sea level by reference to the Anheung Tide Station. Prior to this study, bathymetry was also available from the Nautical Marine Chart (Korea Hydrographic Office, 1987). The compiled bathymetric map (Fig. 3) shows a generally monotonous and flat sea floor. The water depth ranges from 4 m to 15 m, increasing seaward with a low gradient (0.09%). The 3.5 kHz profiles also show a flat seabed smoothed by sediments (Fig. 4).

The sedimentary sequence does not show any distinct subsurface reflectors and appears as one

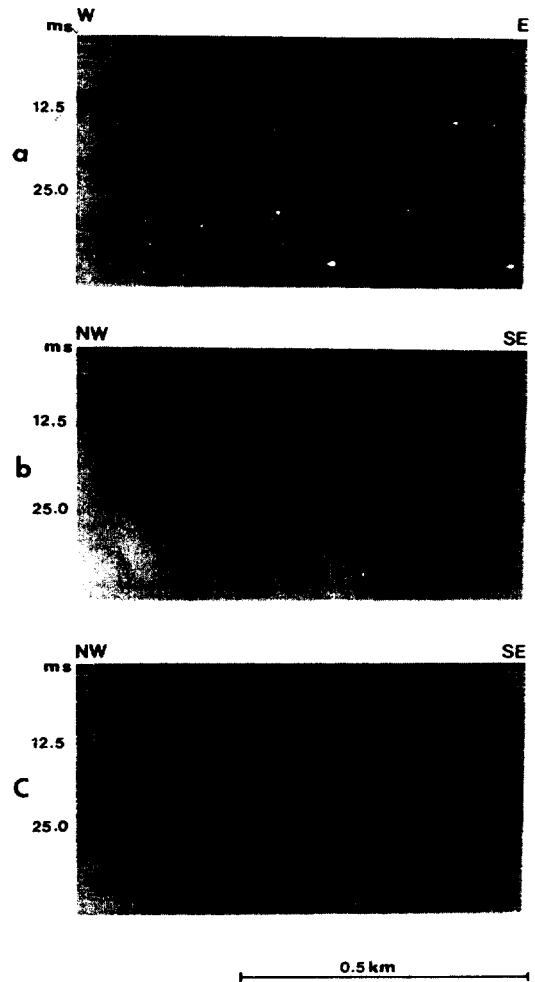


Fig. 4. High-resolution seismic profiles (3.5 kHz) showing flat sea bed and subsurface structures (for location see Fig. 2). SF, sea floor; AB, acoustic basement; M, multiple. Vertical axis is two-way time in milliseconds.

seismic unit. Because of the limit of acoustic penetration into thick coarse deposits, the acoustic basement was not easily identified on seismic profiles. However, the small-scale acoustic impedance contrast reveals the irregular basement beneath the sedimentary sequence, which is traced onto the adjacent land and islands (Fig. 4). The basement deepens toward the middle part of the bay, reaching up to 35 m in depth below sea level. The thickness of sediment sequence above the acoustic basement ranges from 5 to 20 m; thick accumula-

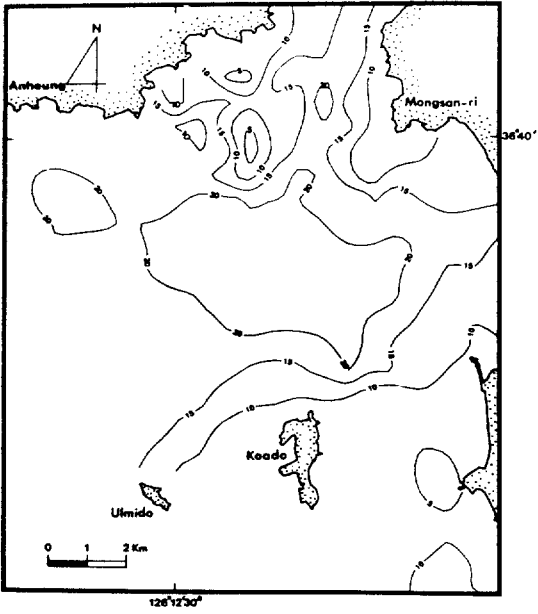


Fig. 5. Isopach map showing the sediment thickness above the acoustic basement (contours in meters).

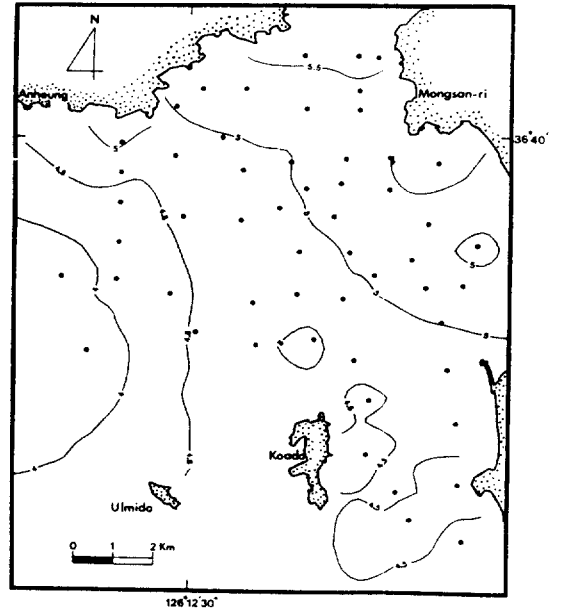


Fig. 7. Distribution of mean grain-size variability in phi scale. Dots are sediment sampling stations.

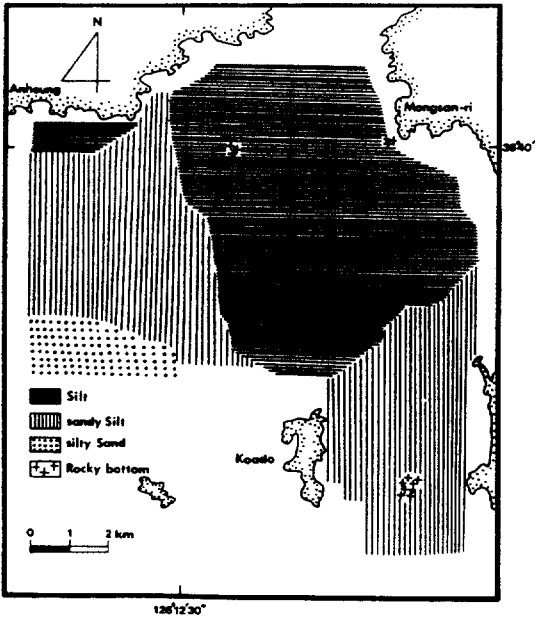


Fig. 6. Distribution map of bottom sediment types. The sediment type is based on the nomenclature suggested by Folk (1954).

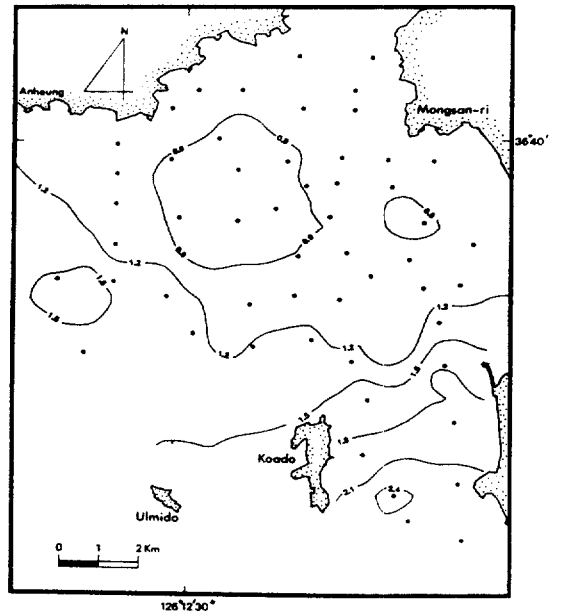


Fig. 8. Distribution of sorting values in phi scale. Dots are sediment sampling stations.

tion occurs in the middle part of the bay whereas the thickness becomes thinner toward the margin (Fig. 5). The irregular surface of the basement rock

is largely modified by sediment accumulation.

SEDIMENT TYPE

Analyses of surface sediments show that silt and

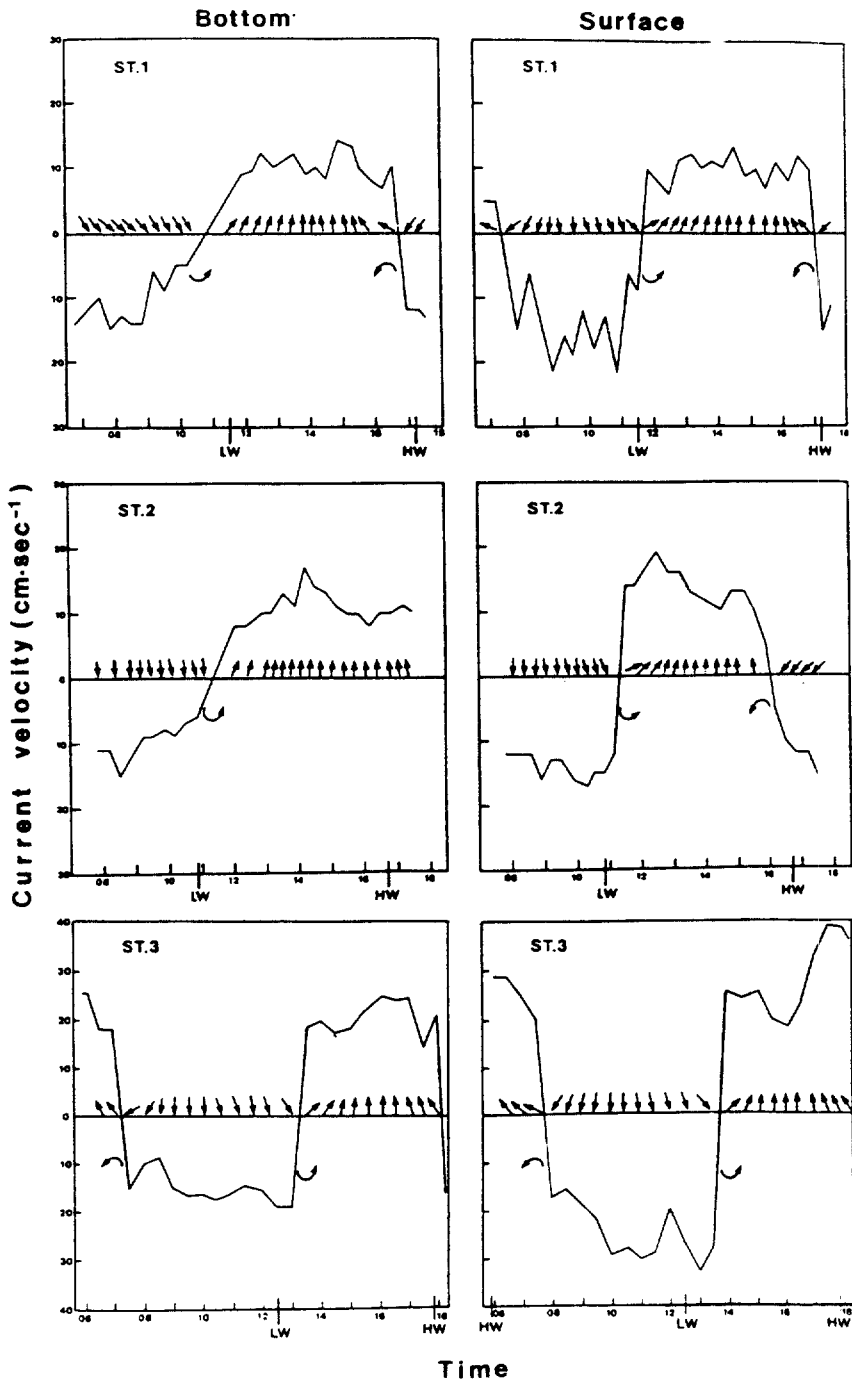


Fig. 9. The variation of velocity and direction of tidal currents at bottom (1 m above the sea bed) and surface with time (for location see Fig. 3). LW: low water, HW: high water. Arrow indicates direction of tidal currents (for details see text).

sandy silt are the dominant sediment types in the bay (Fig. 6). Most of the sediment samples contain

less than 1% gravel and less than 5% clay. Silt dominates the inner and middle part of the bay.

whereas sediment in the outer part of the bay consists mainly of sandy silt and silty sand. The silt content is greater than 90% in the innermost part of the bay and decreases toward the outer part of the bay with increase of the sand content. The sediment samples in the outer part of the bay show the sand content between 10 and 40%. Average grain-size variability in terms of mean diameter also shows the seaward-coarsening trend, ranging from 4 to 5.5 phi (Fig. 7). The sorting value of the sediments ranges from 0.9 to 2.4 phi (Fig. 8). The sediments in the inner and middle part of the bay are relatively better sorted than the sediments in the outer part of the bay.

CURRENT DATA

Figure 9 shows the variations of velocity and direction of surface and bottom tidal currents measured at three stations in the study area. The flow directions of the tidal currents are generally N-NE during flood and S-SW during ebb. The counterclockwise rotation was observed during the change from the ebb to the flood stage and from the flood to the ebb stage. At station 1, the velocity of surface current fluctuates between 5 and 22 cm/sec, showing higher current velocities during ebb than during flood. The bottom-current velocity fluctuates between 5 and 15 cm/sec without any asymmetry in magnitude between flood and ebb. At station 2, the surface-current velocity shows fluctuation between 10 and 19 cm/sec and the bottom-current velocity between 6 and 16 cm/sec. At station 3, the velocity of surface currents, ranging from 16 to 39 cm/sec, is much higher than that of bottom currents. The bottom-current data indicate that the flood-current velocity is generally higher than the ebb-current velocity, with a 27 cm/sec maximum velocity observed during the flood stage.

At each station, the current data show the vertical logarithmic velocity profile during the flow of fully-developed tidal currents. During low current velocities associated with turning of tide, however, the velocity profile is nonlogarithmic. The boundary shear velocity (U_*) and shear stress (τ_0) at

Table 1. The range and mean values of boundary shear velocity (U_*) and boundary shear stress (τ_0) during flood and ebb at each station. For location see Figure 3.

		Flood		Ebb	
		U_*	τ_0	U_*	τ_0
St. 1	Range	0.5-2.0	0.02-0.4	0.8-1.9	0.06-0.38
	Mean	1.0	0.11	1.3	0.17
St. 2	Range	0.8-2.2	0.06-0.48	0.7-2.0	0.04-0.39
	Mean	1.35	0.18	1.2	0.14
St. 3	Range	1.2-3.3	0.14-1.1	0.8-2.3	0.06-0.5
	Mean	1.82	0.33	1.58	0.24

U_* : boundary shear velocity (cm/sec)

τ_0 : boundary shear stress (N/m²)

the seabed were calculated during flood and ebb currents by using the Karman-Prandtl equation

$$\frac{U_1 - U_2}{U_*} = \frac{2.3}{k} (\log Y_1 - \log Y_2)$$

where U_1 and U_2 are the velocities corresponding to the heights Y_1 and Y_2 above the seabed, respectively; k is von Karman's constant (approximately 0.4). It has been proven by numerous researchers that this equation can fairly approximate the velocity distribution in the boundary layer of wide-open tidal channels (Sternberg, 1968, 1972; Smith and McLean, 1977). The boundary shear stress (τ_0) was obtained by the relation, $U_* = (\tau_0/\rho)^{1/2}$, where ρ is the water density. The calculated U_* and τ_0 values are shown in Table 1. At station 1, the U_* (τ_0) value ranges from 0.5 to 2.0 cm/sec (0.02 to 0.4 N/m²) during flood and from 0.8 to 1.9 cm/sec (0.06 to 0.38 N/m²) during ebb. The mean value is somewhat higher during ebb than during flood. At station 2, the flood current shows the U_* (τ_0) range between 0.8 and 2.2 cm/sec (0.06 and 0.48 N/m²) with a mean value of 1.35 cm/sec (0.18 N/m²). The ebb current shows somewhat lower values than the flood current. At station 3, the U_* (τ_0) values are generally higher than those at stations 1 and 2, ranging from 1.2 to 3.3 cm/sec (0.14 to 1.1 N/m²) during flood and from 0.8 to 2.3 cm/sec (0.06 to 0.5 N/m²) during ebb. The mean value is 1.82 cm/sec (0.33 N/m²) and 1.58 cm/sec (0.24 N/m²), respectively. The above results

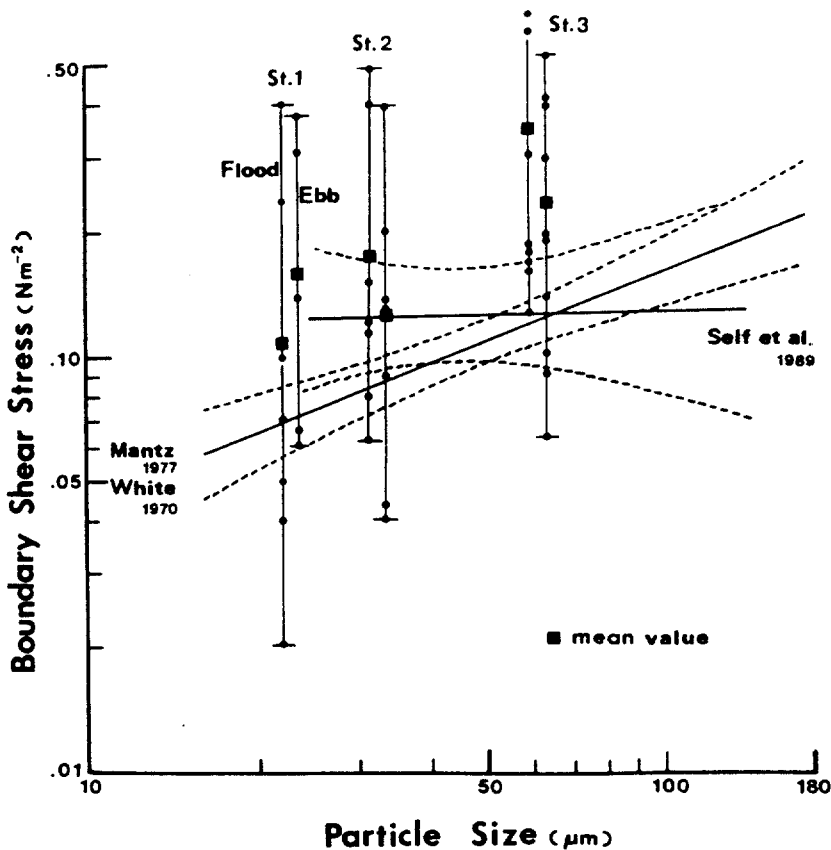


Fig. 10. The range and mean value of boundary shear stress measured in the bay during each phase of tidal currents, plotted on the shear stress-particle size diagram by Self *et al.* (1989). Dots are data points. The diagram shows the critical shear stress of various particle sizes suggested by Self *et al.* (1989), White (1970), and Mantz (1977). Dashed lines are 95% limits for the estimated mean shear stress by these authors.

indicate that the mean values of the measured shear velocities generally decrease shoreward, and that in the outer and middle bay, the values are higher during flood than during ebb.

DISCUSSION AND CONCLUSIONS

The sediment in the bay is comprised mainly of silt with a mean grain size of 4-5.5 phi. According to the coastal mapping project by the Korea Ocean Research and Development Institute (1987), the offshore sediments consist of sand with a mean grain size of 2-3 phi, lacking silt particles. The data suggest a fining trend of sediments northeastward in the bay, which agrees with the flow direction of the tidal currents. The tidal currents

in the bay flow in a N-NE direction during flood and it is largely reversed during ebb. The boundary shear velocity, calculated by the von Karman-Prandtl equation, shows the range from 0.5 to 3.3 cm/sec during flood and from 0.7 to 2.3 cm/sec during ebb. Many experimental studies (Smith and Hopkins, 1972; Cacchione and Drake, 1979; Self *et al.*, 1989) show that coarse silt is eroded and transported when the shear velocity exceeds approximately 1.3 cm/sec. Miller *et al.* (1977) also reported that the threshold shear velocity for cohesionless silt and very fine sand is about 1.0-1.2 cm/sec. Analyses of tidal current data in the bay show that about 70% of the measured bottom shear stresses at three stations exceed the critical shear stresses suggested by Self *et al.* (1989) (Fig.

10). Especially, all values measured at station 3 during flood exceed these suggested critical shear stresses. These data imply that the tidal currents in the bay are strong enough to move the sediment particles.

In this paper, the effect of wind-generated waves is not considered. According to the report by the Korea Ocean Research and Development Institute (1987), waves in the bay are generally 1 m in height and 5-8 sec in period. It is conceivable that with tidal currents superimposed on wave action, a significant portion of silt particles can be reworked and transported in the bay, presumably resulting in a shoreward-fining sediment distribution. A further research is needed to understand the combined influence of tidal currents and wave action in the bay.

ACKNOWLEDGMENTS

This research was partly supported by Korea Ministry of Education (1989). We thank S.K. Hong and K.M. Jang for their valuable assistance in sampling and data analysing. The discussions with Drs. H.J. Kang, J.H. Choi, C.B. Lee, J.K. Oh, and G.S. Chung were very much appreciated.

REFERENCES

- Adams, C. E., J. T. Wells and Y. A. Park, 1990. Internal hydraulics of a sediment-stratified channel flow. *Mar. Geol.*, **95**: 131-145.
- Bloom, A. L. and Y. A. Park, 1985. Holocene sea-level history and tectonic movements, Republic of Korea. *Quater. Res.*, **24**: 77-84.
- Cacchione, D. A. and D. E. Drake, 1979. A new instrument system to investigate sediment dynamics on continental shelves. *Mar. Geol.*, **30**: 299-312.
- Folk, R. L., 1954. The distinction between grain size and mineral composition in sedimentary rock nomenclature. *J. Geol.*, **62**: 334-359.
- Korea Hydrographic Office, 1987. Nautical Marine Chart No. 334 (Kyongyolbiyolto to Anmyeondo). Incheon, Korea.
- Korea Hydrographic Office, 1989. Tide table. Incheon, Korea, 94-95.
- Korea Institute of Energy and Resources, 1981. Geological Map of Korea. Taejon, Korea.
- Korea Ocean Research and Development Institute, 1987. Oceanographic Atlas Series 1, Yellow Sea. Ansan, Korea, 109 pp.
- Mantz, P. A., 1977. Incipient transport of fine grains and flakes by fluids-extended Shield diagram. *Am. Soc. Civ. Eng., J. Hydraul. Div.*, **103**: 601-615.
- Miller, M. C., I. H. McCave and P. D. Komar, 1977. Threshold of sediment motion under unidirectional currents. *Sedimentology*, **24**: 507-527.
- National Geographic Institute of Korea, 1980. Report on coastal mapping project: Anmyoun district. Suwon, Korea, 65 pp.
- Self, R. F. L., A. R. M. Nowell and P. A. Jurnars, 1989. Factors controlling critical shears for deposition and erosion of individual grains. *Mar. Geol.*, **86**: 181-199.
- Smith, J. D. and T. S. Hopkins, 1972. Sediment transport on the continental shelf off Washington and Oregon in light of recent current measurement. In: Shelf Sediment Transport: process and pattern, edited by D. J. P. Swift, D. B. Duane and O. H. Pilkey. Hutchinson and Ross Inc., Dowden, 143-180.
- Smith, J. D. and S. R. McLean, 1977. Spatially averaged flow over a wavy surface. *J. Geophys. Res.*, **82**: 1735-1746.
- Song, Y. O., D. H. Yoo and K. R. Dyer, 1983. Sediment distribution, circulation and provenance in a macrotidal bay: Garolim Bay, Korea. *Mar. Geol.*, **52**: 121-140.
- Sternberg, R. W., 1968. Friction factors in tidal channels with differing bed roughness. *Mar. Geol.*, **6**: 243-260.
- Sternberg, R. W., 1972. Predicting initial motion and bed-load transport of sediment particles in the shallow marine environment. In: Shelf Sediment Transport: process and pattern, edited by D. J. P. Swift, D. B. Duane and O. H. Pilkey. Hutchinson and Ross Inc., Dowden, 61-82.
- White, J. S., 1970. Plane bed thresholds of fine grained sediments. *Nature*, **228**: 152-153.

Received November 28, 1991

Accepted January 6, 1992